NANO LETTERS

Letter

pubs.acs.org/NanoLett

Femtosecond Cooling of Hot Electrons in CdSe Quantum-Well Platelets

Philipp Sippel,[†] Wiebke Albrecht,[‡] Johanna C. van der Bok,[§] Relinde J. A. Van Dijk-Moes,[§] Thomas Hannappel,[∥] Rainer Eichberger,[†] and Daniel Vanmaekelbergh*[,§]

[†]Institute for Solar Fuels, Helmholtz-Zentrum Berlin für Materialien und Energie, Hahn-Meitner-Platz 1, D-14109 Berlin, Germany

[‡]Soft Condensed Matter, Debye Institute for Nanomaterials Science and [§]Condensed Matter and Interfaces, University of Utrecht, Princetonplein 1, 3584 CC Utrecht, The Netherlands

[∥]Institut für Physik, Technische Universität Ilmenau, Postfach 100565, D-98684 Ilmenau, Germany

Supporting Information

ABSTRACT: Semiconductor quantum wells are ubiquitous in high-performance optoelectronic devices such as solar cells and lasers. Understanding and controlling of the (hot) carrier dynamics is essential to optimize their performance. Here, we study hot electron cooling in colloidal CdSe quantum-well nanoplatelets using ultrafast two-photon photoemission spectroscopy at low excitation intensities, resulting typically in 1−5 hot electrons per platelet. We observe initial electron cooling in the femtosecond time domain that slows down with decreasing electron energy and is finished within 2 ps. The cooling is considerably faster at cryogenic temperatures than at room temperature, and at least for the systems that we studied, independent of the thickness of the platelets (here 3−5 CdSe units) and the presence of a CdS shell. The cooling rates that we observe are orders of magnitude faster than reported for similar CdSe platelets under strong excitation. Our results are understood by a classic cooling mechanism with emission of longitudinal optical phonons without a significant influence of the surface.

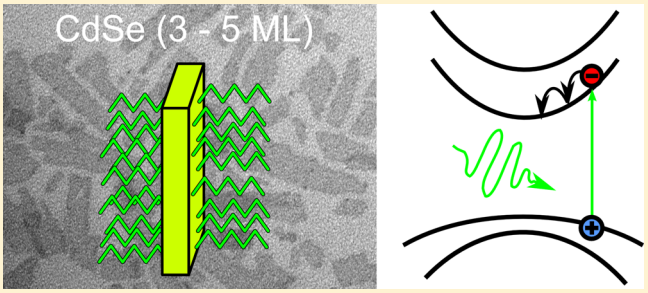

KEYWORDS: *TR-2PPE, platelet, CdSe, hot electron relaxation, photoemission, quantum well*

When a photon is absorbed in a semiconductor crystal with an excess energy with respect to the band gap, the electron (hole) can release this energy in various ways, also depending on the dimensions of the semiconductor. In three-dimensional semiconductors, electrons (holes) can emit phonons to the atomic lattice and "glide" downward (upward) along the quasi-continuous bands until the bottom of the conduction band (top of the valence band) is reached. Typically, longitudinal optical (LO) phonon emission via Fröhlich interaction happens on a femtosecond time scale.[1−3] In principle, this mechanism of cooling by phonon emission also holds for two-dimensional (2D) quantum wells,[4−8] but interfacial reactions can play a role here. In contrast, zero-dimensional quantum dots have discrete energy levels, instead of bands, and the energy difference between two nearest levels is often much larger than the typical phonon energy. Relaxation of electrons from one level to the next thus needs the simultaneous emission of several phonons, which is a slow process. Hence, a "phonon bottleneck" has been predicted for the cooling of hot carriers in quantum dots[9] and has been investigated by transient absorption and time-resolved photoluminescence spectroscopy,[10,11] terahertz spectroscopy,[12] and time-resolved two-photon photoemission spectroscopy (TR-2PPE).[13] It has been found that in these nanometer-sized crystals the phonon bottleneck can be circumvented by Auger-type energy donation from the electron to the hole, followed by fast relaxation of the hole, or by processes involving the ligand or the surface.[10,14−17] The cooling of carriers in bulk and low-dimensional semiconductors is of large interest from a scientific point of view. Furthermore, the knowledge of the cooling rates and how these can be manipulated by structure has direct impact on the design of third generation solar cells, where the collection of hot carriers is a long sought goal, and on semiconductor lasers, where slow cooling would lower the lasing performance.

Here, we present a study of electron cooling in quantum well platelets of the semiconductor CdSe. Marked progress has been made recently in the synthesis of these 2D platelets of (zinc blende) CdSe with lateral dimensions of several tens of nanometers, and thickness of a few unit cells.[18,19] In contrast to 2D systems grown by gas phase deposition, the thickness of these systems is uniform up to the atomic limit[20] and can be controlled by the synthesis. Platelets of CdSe constitute a unique occasion to further the understanding of the

Received: December 8, 2014
Revised: January 29, 2015
Published: March 12, 2015

DOI: 10.1021/nl504706w
Nano Lett. 2015, 15, 2409−2416

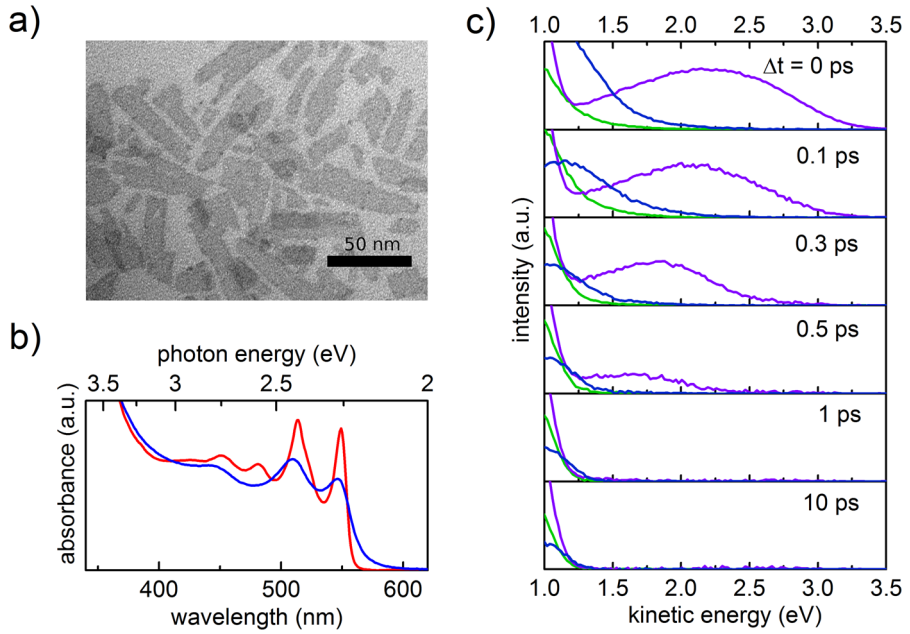

Figure 1. Typical two-photon photoemission experiment on CdSe (3 ML)/CdS core/shell nanoplatelets with different excitation energies, carried out at room temperature. (a) TEM picture of these nanoplatelets. (b) Typical absorption spectrum characterizing the CdSe (3 ML)/CdS core/shell (blue) and the CdSe (5 ML) platelets (red), with the energetically two lowest optical transitions involving the heavy hole and light hole valence bands. (c) Kinetic energy distributions of the photoemitted electrons in a TR-2PPE experiment as a function of time delay between the pump (2.30, 2.60, and 4.52 eV) and the probe pulse (4.52 eV). Green curves: Pump excitation with $h\nu_{pump}$ = 2.30 eV corresponding to the lowest energy transition (cf. panel b), leading to cool electrons at the bottom of the conduction band. Blue curves: excitation with $h\nu_{pump}$ = 2.60 eV leading to hot electrons with a maximum excess energy of 0.35 eV. Purple curves: excitation with $h\nu_{pump}$ = 4.52 eV, leading to hot electrons with a maximum excess energy of 2.27 eV.

optoelectronic properties of 2D semiconductors.[20−25] In that respect, also the cooling of hot carriers has been studied with optical spectroscopy with approximately 5 ps time resolution.[26] Only results obtained at high excitation intensities resulting in about 100 electron hole pairs per platelet could be resolved with the cooling taking place in the 10 ps time regime. This agrees with previous results obtained for other quantum well systems and even bulk CdSe,[2,5] where electron relaxation on a similar time scale was measured. In view of intrinsic electron−phonon scattering that occurs on a femtosecond time scale, this slow cooling has been attributed to the so-called LO phonon bottleneck (not to be mixed up with the phonon bottleneck in quantum dots); the high density of hot carriers generate a high density of LO phonons (not in thermal equilibrium with the lattice), which are either reabsorbed by the electrons, diffuse away, or slowly decay to phonons of lower energy.[1,27,28] We remark that there is still very little experimental data available for intrinsic cooling dynamics of a hot electron gas in the low-density limit in a two-dimensional semiconductor quantum well.

Our method of choice for the study of the electron cooling in CdSe quantum-well platelets is TR-2PPE and described in detail in the Supporting Information section. This technique monitors the temporal evolution of a photoinduced electron distribution time, as well as energy-resolved, in a single experiment. The time resolution is sub-40 fs and thus in the range of the typical release time of a single LO phonon by a hot electron. Because the technique is sensitive to electrons only, it is complementary to, for example, hot-luminescence spectroscopy that monitors the total energy of an electron−hole pair. Moreover, the experiments are carried out at low excitation intensities, for which the average exciton density per platelet is between about 1 and 5 electron−hole pairs per platelet, depending on the sample and the excitation wavelength. Finally, TR-2PPE requests that the CdSe platelets are in contact with an electrode. In such a way, the carrier cooling is studied in an all-solid device that resembles practical optoelectronic devices such as a solar cell, or an electrically driven laser.

The synthesis of CdSe platelets is very versatile and hence we could investigate atomically precise platelets of different well-defined thickness. The thickness is best assigned by the first absorption/emission peak, which was at 2.25 and 2.67 eV, respectively, for two specific bare CdSe platelets ensembles in this study. While recent publications[29] indicate that these bandgaps correspond to 5, respectively, 3 monolayers (ML), we remark that there is still some uncertainty over the exact number of CdSe units.[18,22,29] The platelets are capped with organic ligands or enclosed by a thin shell of the higher band gap semiconductor CdS. The band offset for colloidal CdSe/CdS heterostructures is mostly to be found in the valence bands, while the conduction bands show little or no offset and the electrons are thus delocalized over the core and the shell, while the holes are confined in the CdSe core.[30−33] The versatility and the unique control in platelet synthesis offer an exclusive possibility to study the effect of the surface and interfaces on the cooling dynamics in 2D systems and to compare colloidal quantum wells with their solid-state counterparts, that is, multiple quantum-well structures prepared by gas-phase deposition.

The principle of TR-2PPE is to photogenerate electrons with certain excess energy by applying a short laser pulse, called the pump pulse and subsequently lift these electrons beyond the vacuum level with a second, delayed laser pulse (the probe

DOI: 10.1021/nl504706w
Nano Lett. 2015, 15, 2409−2416

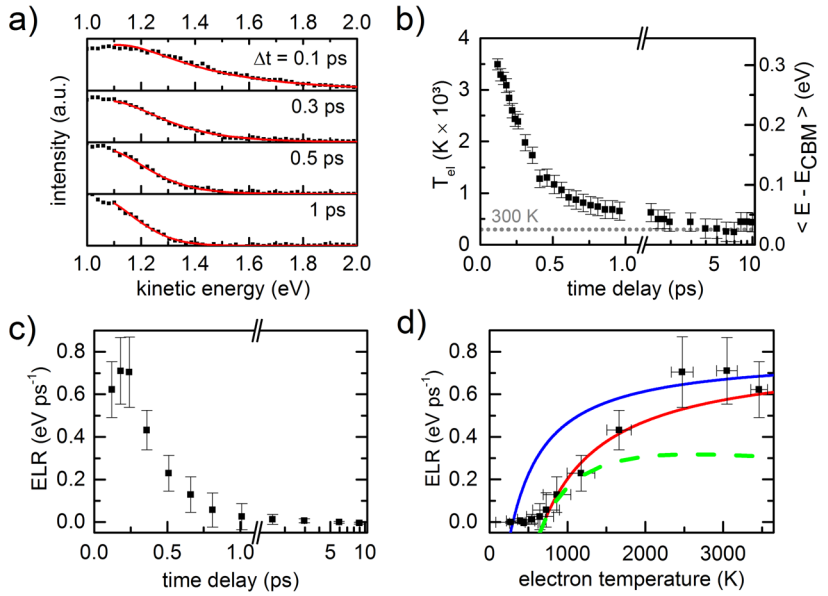

Figure 2. Cooling of the electron distribution, photoexcited with $h\nu_{pump}$ = 2.60 eV at CdSe (3 ML)/CdS core/shell platelets (cf. blue spectra in Figure 1c). (a) Kinetic energy spectra for different pump probe delays (black symbols) with fits of the high-kinetic-energy tails based on a stepwise DOS and Fermi–Dirac statistic (red lines). (b) Resulting electron temperature as a function of time delay Δt, obtained from the fits in (a) (left ordinate) and the corresponding average electron energy with respect to the CBM (right ordinate). (c) Average ELR per electron as a function of time delay, obtained by calculating the derivation of the average energy curve in (b). (d) ELR as a function of electron temperature (black squares), obtained by combining (b) and (c). Result of eq 3 for τ = 33 fs with T_{lat} = 700 K (red solid line) and T_{lat} = 300 K (blue solid line). For the former case, also the result from a numeric simulation according to refs 39 and 40. is shown (green dashed line).

pulse) with high photon energy ($h\nu_{probe}$ = 4.52 eV) so that the kinetic energy of the photoemitted electrons can be measured. The kinetic energy depends on the original binding energy of the electron and the measured energy distribution thus reflects the energy distribution of the photogenerated electrons within the semiconductor apart from a shift on the energy axis that depends on the photon energy and the vacuum energy of the sample. Recording spectra for different time delays between the pump and probe pulses thus allows to measure the temporal evolution of the electron distribution after photoexcitation. In Figure 1, we present typical results obtained with CdSe(3 ML)/CdS core/shell platelets. A transmission electron microscopy (TEM) picture of the platelets is presented in Figure 1a; the platelets are nearly flat 2D systems with lateral dimensions of about 10 × 60 nm; presumably the thickness of the CdSe is 3 ML, shelled with 2 ML of CdS. The first absorption and emission peak is situated at 550 nm (2.25 eV), as shown in Figure 1b. Figure 1c shows the kinetic energy of the emitted electrons with respect to the vacuum level of the sample as a function of the time delay between pump and probe for $h\nu_{pump}$ = 2.30 eV (540 nm), $h\nu_{pump}$ = 2.60 eV (478 nm), and $h\nu_{pump}$ = 4.52 eV (274 nm). With $h\nu_{pump}$ = 2.30 eV (first peak of the absorption spectrum) electrons are excited to the bottom of the conduction band (CB). The green plots show the corresponding kinetic energy of electrons that are photoemitted from the bottom of the CB, convoluted with the energy resolution of the setup (approximately[13] 0.2 eV), and serve as a reference. Deconvolution yields that the bottom of the CB is situated approximately 3.55 eV below the vacuum level of the sample as discussed further below.

The blue and purple curves represent the 2PPE results with $h\nu_{pump}$ = 2.60 eV and $h\nu_{pump}$ = 4.52 eV, respectively, leading to hot electrons with an initial maximum excess energy of 0.35 and 2.27 eV above the conduction band minimum (CBM), respectively. The average excess energy of the photoexcited electrons, however, is considerably lower due to the dispersion of the heavy hole valence band and transitions from lower lying valence bands. Spectral features related to transitions from the different hole-bands could not be resolved because the spectral resolution is limited to approximately 0.2 eV. The signal at the low kinetic energy edge (Ekin < 1.1 eV) must be treated with care as it contains large amounts of secondary electrons. These are electrons that have lost parts of their kinetic energy by inelastic scattering processes. This is especially pronounced for excitation with $h\nu_{pump}$ = 4.52 eV. As expected, the two different pump energies result in very different electron distributions at short time delays. Overall, the distributions change fast in the <0.5 ps time domain and more slowly on later times; at Δt = 1 ps, the electrons have nearly completely cooled down to the CBM, in accordance to TR-2PPE measurements of the electron dynamics at 3D semiconductor interfaces.[34]

We now focus in detail on the cooling of electrons pumped with $h\nu_{pump}$ = 2.60 eV, that is, that have a maximum excess energy of 0.35 eV; Figure 2a shows the kinetic energy distribution of the CdSe (3 ML)/CdS core/shell sample, with normalized intensity. The electron distribution of the hot electron gas (consisting of ~5 electrons per platelet; see Supporting Information) can be described by an electron temperature T_e, which is a result of equilibration by very fast electron–electron scattering that happens typically within less than 100 fs.[35−37] This electron temperature was extracted by fitting the high-energy tail of the kinetic energy spectra with the product of the Fermi–Dirac distribution function and the steplike density of states (DOS) of a quantum well with infinite barriers, 1.5 nm thickness and an effective mass[38] of m_{eff} = 0.13 m_e. Another important parameter is the kinetic energy E_{kin}^{CBM}, corresponding to photoemitted electrons that stem from the CBM. For Δt > 150 fs, we obtained clear fitting results with E_{kin}^{CBM} = 0.97 eV. From

DOI: 10.1021/nl504706w
Nano Lett. 2015, 15, 2409−2416

$$E_{kin}^{CBM} = E_{CBM} - h\nu \quad (1)$$

we depict that the CBM is located 3.55 eV below the vacuum level. It should be remarked that this value holds for the oleic acid capped platelets studied here and that different capping can shift the band edges.

For $\Delta t < 150$ fs, there is a small but considerable deviation between the experimental data and our fit (see Figure 2a; spectrum at $\Delta t = 0.1$ ps), compared to the almost perfect fit for larger time delays. This might indicate that the electron distribution has not developed to a state of equilibrium within this time interval. However, it could also be related to our DOS approximation that becomes arguable for higher electron energies, as present for early time delays. The electron temperature extracted with the fit is plotted in Figure 2b for $\Delta t > 150$ fs as a function of the time delay between pump and probe. We see that T_e drops from 3500 K at $\Delta t = 150$ fs to about 650 K within 1 ps, followed by a significantly slower relaxation on the picosecond time scale. For an accurate determination of the electron temperature, it is necessary to take into account that the energy resolution of the setup is rather coarse compared to the width of an electron distribution at low electron temperatures, which, for example, is only $\Delta_{ED} = k_B T_e \approx 0.026$ eV for $T_e = 300$ K. In the fit, this was included by convolution with a corresponding Gaussian and with $\Delta_{res}^{fwhm} = 0.12$ eV the electron temperature asymptotically approaches ~300 K for long pump probe delays. We note that the energy resolution is subject to an unavoidable uncertainty due to several broadening influences[13,41] and thus the electron temperature as presented here might be slightly underestimated.

Now, we translate this electron temperature into the average electron energy with respect to the CBM, given by

$$\langle E - E_{CBM} \rangle = k_B T_e \quad (2)$$

for a 2D DOS, based on the infinite quantum well when approximating the Fermi–Dirac statistics with a Maxwell–Boltzmann distribution. The average energy with respect to the CBM is shown on the right-hand ordinate in Figure 2b and the error bars represent the statistic error due to the finite electron count rate. $T_e = 3500$ K corresponds to an average energy of ~0.3 eV, while the maximum excess energy that could be reached in this experiment is 0.35 eV, given by the difference between the pump photon energy and the band gap. The fact that we observe a lower value is presumably caused by optical transitions from the lower lying light hole band and by a small part of the excess photon energy used to excite holes. By calculating the derivation of the average energy, we can now deduce the time-dependent average energy loss rate (ELR) per electron $\langle -dE/dt \rangle$ as shown in Figure 2c. Furthermore, by combining this with the time-dependent electron temperature, shown in Figure 2b, we obtained the ELR as a function of the electron temperature (plotted in Figure 2d) and find that it is strongly reduced with decreasing electron temperature.

In this temperature regime, the transfer of energy from a hot electron gas to the lattice in polar semiconductors is dominated by the emission of longitudinal optical (LO) phonons. For quantum wells with infinite barriers, Ridley has approached this case theoretically,[39,40] assuming a bulklike LO phonon band with a constant phonon energy $\hbar\omega_{LO}$. For the lowest sub-band and for $q_{max}L \geq 4$, where q_{max} is the maximum momentum of the emitted/absorbed phonon and L is the thickness of the quantum well, the phonon emission and absorption rates can be approximated as constant.[39] However, only electrons with $E - E_{CBM} \geq \hbar\omega_{LO}$ can emit phonons, as otherwise there are no states available for the scattered electrons. On the basis of this we calculate the average ELR per electron as a function of electron temperature[3] and obtain

$$\left\langle -\frac{dE}{dt} \right\rangle = \frac{\hbar\omega_{LO}}{\tau} \exp\left(-\frac{\hbar\omega_{LO}}{k_B T_e}\right) \times \frac{\exp\left(\frac{\hbar\omega_{LO}}{k_B T_{lat}}\right) - \exp\left(\frac{\hbar\omega_{LO}}{k_B T_e}\right)}{\exp\left(\frac{\hbar\omega_{LO}}{k_B T_{lat}}\right) - 1} \quad (3)$$

Here, τ is the constant electron phonon scattering time and T_{lat} is the lattice temperature. For $T_{lat} \to 0$ the fraction on the right-hand side approaches unity and eq 3 becomes a relation, well-known from textbooks[3] and also valid for bulk semiconductors. The blue line in Figure 2d shows the result of eq 3 for $\tau = 33$ fs, $T_{lat} = 293$ K, and $\hbar\omega_{LO} = 26$ meV, which is the LO phonon energy for CdSe.[38] For $T_e > 2000$ K, this agrees with the measured data, but for $T_e < 2000$ K the measured ELR is lower than the calculated curve and furthermore drops drastically at $T_e \approx 700$ K. This indicates that the cooling via LO phonon emission is suppressed, either for electron temperatures <700 K in general or after a certain amount of energy has been transferred to the lattice, for example, due to the buildup of a hot phonon distribution that slows down the cooling process after T_e has reached about 700 K.

For comparison, we also plotted the result of eq 3 for the same parameters as above, but $T_{lat} = 700$ K (red line in Figure 2d). Here, the agreement is quite good for $T_e < 2000$ K. Since in our case the wells are pretty thin and $q_{max}L \geq 4$ is not fulfilled, we furthermore calculated the ELR numerically, according to Riddoch and Ridley,[40] choosing CdSe parameters from standard compendia[38] ($\varepsilon_\infty = 6.3$; $\varepsilon_s = 9.3$; $m_{eff} = 0.13\ m_e$) with $T_{lat} = 700$ K (green dashed line in Figure 2d). This also agrees with the measured data for $T_e < 1500$ K but strongly underestimates the measured ELR for higher electron temperatures. We remark that the parameters, used here, apply for bulk CdSe but might be significantly different for thin nanoplatelets with CdS shell.

Now, we discuss the effect of the lattice temperature on the electron cooling dynamics by comparing TR-2PPE measurements at room temperature to those at 25 K (Figure 3). We show results obtained with CdSe (3 ML) platelets (absorption peak at 2.67 eV) for a pump photon energy of 4.52 eV. At this photon energy, electrons with high excess energy are created, allowing us to monitor the relaxation process over a wider energy range and at excitation densities of ~1 exciton per nanoplatelet. In Figure 3a, the kinetic energy distribution is presented for different pump–probe delays.

For single electrons, the electron temperature is not a proper quantity. Therefore, we calculate the average kinetic energy of the photoemitted electrons instead, given by

$$\langle E_{kin} \rangle = \frac{\sum E_{kin,i} n_i}{\sum n_i} \quad (4)$$

where n_i is the number of photoemitted electrons with $E_{kin,i}$. The resulting curves are shown in Figure 3b. To reduce the influence of secondary electrons, that have a high count rate at low kinetic energies, electrons with $E_{kin} < 1.2$ eV were neglected. For a Maxwell–Boltzmann distribution and a

DOI: 10.1021/nl504706w
Nano Lett. 2015, 15, 2409–2416

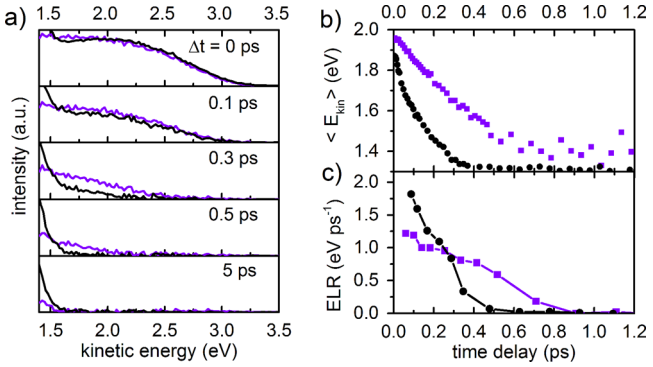

Figure 3. Evolution of the average electron energy and energy loss rates (ELRs) in CdSe nanoplatelets at different lattice temperatures T_{lat} = 293 K (purple curves) and T_{lat} = 25 K (black curves) after photoexcitation with $h\nu_{pump}$= 4.52 eV. (a) Kinetic energy spectra for different pump probe delays. (b) Average kinetic energy, obtained from (a) as a function of time delay. To minimize the influence of secondary electrons, electrons with E_{kin} < 1.2 eV were neglected. (c) Resulting ELRs, obtained by calculating the derivations of the curves in (b).

constant 2D DOS, this just leads to a constant offset of the average kinetic energy and

$$\langle E_{kin}\rangle = \langle E - E_{CBM}\rangle + C \quad (5)$$

where C is a constant that contains this offset, the photon energy, and the vacuum level of the sample. Thus, as before, derivation of $\langle E_{kin}\rangle$ yields the time-dependent average ELR, which is shown in Figure 3c for both temperatures. Error bars would be of comparable size as in Figure 2 but are omitted here and in the following for the sake of clarity. It is obvious that in the first 0.3 ps, where most of the relaxation occurs, the ELR for the measurement at T_{lat} = 25 K is significantly higher than for the measurement at room temperature. At low temperatures, less phonons are thermally activated and consequently less phonons are absorbed by the electrons, leading to a faster relaxation. It should be kept in mind that lowering the lattice temperature not only freezes phonon modes but also can influence the electronic properties of the material. According to Tessier et al., the band gap should increase by approximately 0.05 eV,[42] when cooling NPs of similar size down to 25 K. Thus, at 25 K lattice temperature the electrons will have slightly less excess energy that in turn should lead to a slower relaxation, which is in contrast to the faster measured relaxation. However, the drastic increase in ELR cannot be explained with the model in eq 3 as for single electrons the distribution approach does not hold anymore. Also, the high excess energy initially leads to very high ELRs, that reach ~1.8 eV ps^{-1} for T_{lat} = 25 K, resulting in phonon emission rates >1/17 fs^{-1} which is faster than the values we found in the measurements, shown in Figure 2. This indicates alternative decay pathways such as the emission of transverse optical phonons and LO phonon emission via deformation potential scattering that become dominant for high excess energy, while the probability for polar optical mode scattering decreases due to the electrostatic nature of the interaction as high q values are required for the scattering events.[43] Furthermore, intersubband scattering between the n = 1 and the n = 2 energy levels would have to be considered for a precise theoretical description at such high excess energies.

In order to investigate the effect of the thickness of the quantum-well platelets and the surface chemistry on the electron energy loss mechanism(s), we performed measurements on different samples; the results are summarized in Figure 4. All measurements were performed with a pump

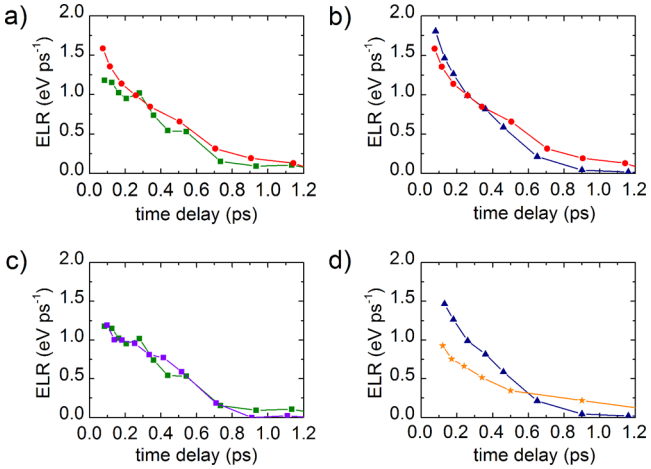

Figure 4. Comparison of the ELRs as a function of time delay, measured on CdSe platelets of variable thickness, with different capping, and with and without a CdS shell. Finally, results for CdSe quantum dots are shown for comparison. The measurements were performed at room temperature with $h\nu_{pump}$ = 4.52 eV excitation energy. (a) CdSe (3 ML)/CdS core/shell platelets (red curve) compared with CdSe (3 ML) platelets (green curve), both capped with OA. (b) CdSe (3 ML)/CdS core/shell platelets (red curve) compared with CdSe (5 ML) platelets (blue curve), both capped with OA. (c) CdSe (3 ML) platelets with OA capping (green curve) compared with identical platelets, capped with HDT (purple curve). (d) CdSe quantum dots of 3.5 nm diameter with HDT ligands, preventing Auger relaxation via the VB holes (orange curve), compared to CdSe (5 ML) platelets with OA capping (blue curve).

photon energy of $h\nu_{pump}$ = 4.52 eV and the shown ELRs were deduced in the same fashion as done above for the measurements with different lattice temperatures.

Figure 4a shows the ELR for CdSe (3 ML) samples with and without CdS shell. Overall, we find a strikingly similar ELR in nearly the entire time window, except for the first 200 fs. We note that the first absorption feature of the core/shell system is considerably red shifted with respect to the core-only platelets. In order to avoid this, we also compare results for CdSe (5 ML) platelets with the CdSe (3 ML)/CdS core/shell platelets in Figure 4b. As shown in Figure 1b, both these samples have their first absorption resonance at nearly the same energy, which means that also the initial excess kinetic energy of the photoexcited electrons should be similar. In this case, the ELR is nearly identical for the entire time span in which cooling takes place. The results, presented in Figure 4a and b (and several repetitions of these experiments with other samples), show that the ELR in the CdSe platelets does not change by the presence of a CdS shell around the platelets.

In Figure 4c we investigate whether the trapping of valence band holes at the surface, that prevents electron-to-hole Auger relaxation, has any effect on the electron cooling. We compared bare CdSe (3 ML) platelets with oleic acid (OA) capping with the same platelets, capped with 1,6-hexanedithiol (HDT); the latter ligands have been shown to act as hole trap[44] preventing energy donation from the electron to the hole in CdSe quantum-dot nanocrystals.[13,45,46] As we expect that the surface chemistry of the facets of the platelets is very similar to that of

DOI: 10.1021/nl504706w
Nano Lett. 2015, 15, 2409−2416

nanocrystals, we anticipate that holes are trapped at the surface of thiol-capped platelets as well. An indication for that is presented in ref 19, where it was reported that the photoluminescence quantum yield drops to half the value if the platelets are recapped with thiols. It is obvious from Figure 4c that in the case of platelets we find no difference in ELR between the samples, which indicates that Auger-type electron cooling is not important in the case of 2D platelets. This mechanism seems to be unable to compete with direct electron decay via the conduction band by LO-phonon emission.

In Figure 4d, we compare the ELR of CdSe (5 ML) nanoplatelets with that of CdSe quantum dots of 3.5 nm diameter with their lowest optical transition (2.18 eV) being nearly identical to that of the nanoplatelets (2.25 eV). We thereby have used HDT as capping for the quantum dots to suppress the Auger-type cooling pathway. Our results show that the ELR for the platelets is significantly higher and hence cooling via the continuous 2D conduction band is much faster than the multiphonon transition between discrete energy levels in the quantum dots. This effect is even more pronounced when comparing our results on nanoplatelets with measurements on CdSe quantum dots with hole scavenging ligands, where the second lowest electron level $1P_e$ is photoexcited resonantly.[45,47,13] This highlights the effect of the "quantum" phonon bottleneck[48] that has been predicted for semiconductors with quantum confinement in all three dimensions as illustrated in Figure 5.

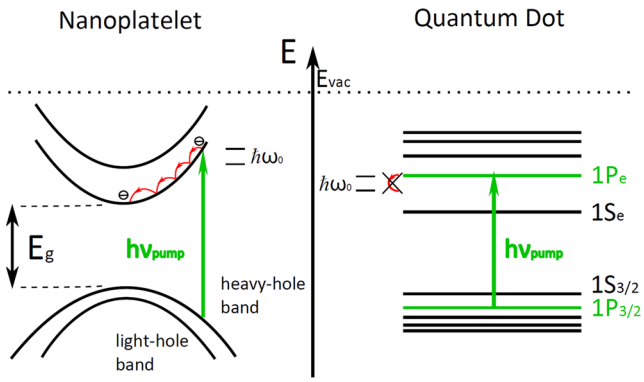

Figure 5. Comparison of the electron relaxation in nanoplatelets (left) and quantum dots (right). Nanoplatelets are confined only in one dimension and thus have a continuous DOS. Consequently, electrons can reach the CBM by the emission of single LO phonons. In quantum dots, the energetic distance between the electronic levels is larger than the LO phonon energy and electron cooling via the emission of single phonons is suppressed.

The results that we presented here show that in CdSe platelets of 3−5 ML thickness, hot electrons lose most of their excess kinetic energy in the first picosecond after excitation. The ensuing further cooling is markedly slower and the minimum of the CB is reached within 10 ps. The energy loss rate (ELR), thereby, strongly depends on the average energy or temperature of the electron gas in the platelets. The results show no measurable dependence on platelets thickness and the surface layer around the platelets be it different capping molecules or a thin layer of CdS. The nature of our measurement does not allow the evaluation of minor changes in relaxation rate, for example, due to different DOS in the lowest subband[39,49] or due to a change in the dielectric constant by variation of the capping. Nevertheless, if the major decay mechanisms were surface related our experiments should show significant variations in the measured ELRs as, for example, found for CdSe quantum dots.[10,47,50] We therefore conclude that surface-related decay mechanisms play a secondary role and instead fast phonon-assisted cooling within the platelets is the dominant decay mechanism. Also no evidence for Auger-type electron-to-hole energy donation was found in experiments, where the oleic acid capping was replaced with a thiol capping that is known to trap holes. Instead the ELR does not change notably, indicating that electron−phonon scattering via the Fröhlich-interaction happens on a significantly faster time scale.

All the above results imply that the electron cooling along the 2D bands of the quantum-well platelets by emission of LO phonons is the main cooling mechanism. For the state directly after photoexcitation, the dependence of the ELR on the electron temperature can be described well with a simplified model for polar-mode scattering in 2D systems. Good agreement is found with a scattering rate of τ = 33 fs, which is close to the 15 fs calculated for Fröhlich interaction in 2D systems, using basic assumptions[3] and standard CdSe parameters.[38] However, if we assume a lattice temperature of T_{lat} = 293 K, this model cannot describe a drastic break down in ELR that we measure for T_e < 700 K, indicating a strong reduction of the net LO phonon emission rate. While this might be explained by a strong reduction of the LO phonon emission rate for electrons with T_e < 700 K, we believe that this is rather related due to an increase of LO phonon absorption, caused by the buildup of a distribution of hot LO phonons during the cooling process: by reabsorption of these hot phonons the cooling is considerably slowed down for T_e < 700 K. In fact, when assuming a lattice temperature of T_{lat} = 700 K we achieve good quantitative agreement between model and data in this electron temperature range.

Slow decay attributed to the hot phonon bottleneck is commonly reported for experiments with 2D and 3D CdSe; the ELR then strongly depends on the lifetime of the optical phonons that is estimated to be 6−9 ps.[1] In this respect, Vengurlekar et al. reported that the cooling rates in bulk CdSe at cryogenic temperatures[1] depended strongly on the excitation intensity with the ELRs being more than an order of magnitude lower than measured in our experiments. Pelton et al. also performed time-resolved photoluminescence measurements on CdSe nanoplatelets,[26] and reported a decay constant of several tens of picoseconds for the electron cooling from 700 K to room temperature, hence, much slower than observed in our experiments. The difference must be caused by the excitation intensities resulting in >100 excitons/platelet in ref 26, while in our case the excitation density leads to a maximum of 5 excitons/platelet, as the ELR reduction due to hot phonons increases with increasing excitation density.[1] The authors of ref 26 also remark that their setup was limited to a time resolution of about 5 ps and fast initial cooling at low excitation densities could thus not be resolved.

To conclude, we studied electron cooling in CdSe platelets using TR-2PPE with a time-resolution of sub-40 fs. We used very low pump intensity, leading to 1−5 hot electrons per platelet. We observe major cooling in the time regime below 1 ps. Only in the later stage of the cooling process, the cooling slows down, very probably due to reabsorption of hot phonons. Furthermore, the cooling rate increases with lower lattice temperature. In the CdSe and CdSe/CdS platelets that we studied, the thickness of the platelets (3 to 5 CdSe units) and

DOI: 10.1021/nl504706w
Nano Lett. 2015, 15, 2409−2416

the CdS shell (1−2 units) did not markedly influence the cooling kinetics. Our results can be largely explained by hot electron cooling in parabolic bands via LO-phonon emission. Our results are important for lasing devices based on CdSe platelets[51] and for third generation designs in photovoltaics, aimed at directly collecting hot carriers.[9] In a broader sense, our results form another indication that chemically prepared CdSe nanoplatelets behave as genuine 2D quantum wells.

■ ASSOCIATED CONTENT

Supporting Information

The SI contains information about the synthesis of CdSe nanoplatelets of different thickness, the formation of the electron-emitting electrodes with CdSe platelets, the TR-2PPE setup and the determination of the excitation density per platelet. This material is available free of charge via the Internet at http://pubs.acs.org.

■ AUTHOR INFORMATION

Corresponding Author

*E-mail: d.vanmaekelbergh@uu.nl.

Author Contributions

The manuscript was written through contributions of all authors. All authors have given approval to the final version of the manuscript.

Notes

The authors declare no competing financial interest.

■ ACKNOWLEDGMENTS

P.S., R.E., and T.H. want to thank the BMBF (Project No.03SF0404A) for financial support.

■ REFERENCES

(1) Vengurlekar, A. S.; Prabhu, S. S.; Roy, S. K.; Shah, J. *Phys. Rev. B* **1994**, *50*, 15461−15464.
(2) Cai, W.; Marchetti, M. C.; Lax, M. *Phys. Rev. B* **1986**, *34*, 8573−8580.
(3) Shah, J. *Ultrafast Spectroscopy of Semiconductors and Semiconductor Nanostructures*; Springer: Berlin, 1999.
(4) Lobentanzer, H.; Stolz, W.; Nagle, J.; Ploog, K. *Phys. Rev. B* **1989**, *39*, 5234−5244.
(5) Rosenwaks, Y.; Hanna, M. C.; Levi, D. H.; Szmyd, D. M.; Ahrenkiel, R. K.; Nozik, A. J. *Phys. Rev. B* **1993**, *48*, 14675−14678.
(6) Yang, C. H.; Carlson-Swindle, J. M.; Lyon, S. A.; Worlock, J. M. *Phys. Rev. Lett.* **1985**, *55*, 2359−2361.
(7) Ryan, J. F.; Taylor, R. A.; Turberfield, A. J.; Maciel, A.; Worlock, J. M.; Gossard, A. C.; Wiegmann, W. *Phys. Rev. Lett.* **1984**, *53*, 1841−1844.
(8) Snow, P. A.; Westland, D. J.; Ryan, J. F.; Kerr, T.; Munekata, H.; Chang, L. L. *Superlattices Microstruct.* **1989**, *5*, 595−598.
(9) Nozik, A. *Phys. E (Amsterdam, Neth.)* **2002**, *14*, 115−120.
(10) Pandey, A.; Guyot-Sionnest, P. *Science* **2008**, *322*, 929−932.
(11) Klimov, V. I.; Bawendi, M. G. *MRS Bull.* **2001**, *26*, 998−1004.
(12) Hendry, E.; Koeberg, M.; Wang, F.; Zhang, H.; de Mello Donegá, C.; Vanmaekelbergh, D.; Bonn, M. *Phys. Rev. Lett.* **2006**, *96*, 057408.
(13) Sippel, P.; Albrecht, W.; Mitoraj, D.; Eichberger, R.; Hannappel, T.; Vanmaekelbergh, D. *Nano Lett.* **2013**, *13*, 1655−1661.
(14) Efros, A. L.; Kharchenko, V. A.; Rosen, M. *Solid State Commun.* **1995**, *93*, 281−284.
(15) Cooney, R. R.; Sewall, S. L.; Dias, E. A.; Sagar, D. M.; Anderson, K. E. H.; Kambhampati, P. *Phys. Rev. B* **2007**, *75*, 245311.
(16) Kambhampati, P. *Acc. Chem. Res.* **2010**, *44*, 1−13.
(17) Kambhampati, P. *J. Phys. Chem. C* **2011**, *115*, 22089−22109.
(18) Ithurria, S.; Tessier, M. D.; Mahler, B.; Lobo, R. P. S. M.; Dubertret, B.; Efros, A. L. *Nat. Mater.* **2011**, *10*, 936−941.
(19) Mahler, B.; Nadal, B.; Bouet, C.; Patriarche, G.; Dubertret, B. *J. Am. Chem. Soc.* **2012**, *134*, 18591−18598.
(20) Tessier, M. D.; Javaux, C.; Maksimovic, I.; Loriette, V.; Dubertret, B. *ACS Nano* **2012**, *6*, 6751−6758.
(21) Javaux, C.; Mahler, B.; Dubertret, B.; Shabaev, A.; Rodina, A. V.; Efros, A. L.; Yakovlev, D. R.; Liu, F.; Bayer, M.; Camps, G.; Biadala, L.; Buil, S.; Quelin, X.; Hermier, J.-P. *Nat. Nanotechnol.* **2013**, *8*, 206−212.
(22) Benchamekh, R.; Gippius, N. A.; Even, J.; Nestoklon, M. O.; Jancu, J.-M.; Ithurria, S.; Dubertret, B.; Efros, A. L.; Voisin, P. *Phys. Rev. B* **2014**, *89*, 035307.
(23) Lhuillier, E.; Robin, A.; Ithurria, S.; Aubin, H.; Dubertret, B. *Nano Lett.* **2014**, *14*, 2715−2719.
(24) Biadala, L.; Liu, F.; Tessier, M. D.; Yakovlev, D. R.; Dubertret, B.; Bayer, M. *Nano Lett.* **2014**, *14*, 1134−1139.
(25) Kunneman, L. T.; Tessier, M. D.; Heuclin, H.; Dubertret, B.; Aulin, Y. V.; Grozema, F. C.; Schins, J. M.; Siebbeles, L. D. A. *J. Phys. Chem. Lett.* **2013**, *4*, 3574−3578.
(26) Pelton, M.; Ithurria, S.; Schaller, R. D.; Dolzhnikov, D. S.; Talapin, D. V. *Nano Lett.* **2012**, *12*, 6158−6163.
(27) Pugnet, M.; Collet, J.; Cornet, A. *Solid State Commun.* **1981**, *38*, 531−536.
(28) Žukauskas, A. *Phys. Rev. B* **1998**, *57*, 15337−15344.
(29) Dijksman, A. T.; Dubertret, B. *Phys. Status Solidi B* **2014**, *251*, 537−541.
(30) Borys, N. J.; Walter, M. J.; Huang, J.; Talapin, D. V.; Lupton, J. M. *Science* **2010**, *330*, 1371−1374.
(31) Lupo, M. G.; Della Sala, F.; Carbone, L.; Zavelani-Rossi, M.; Fiore, A.; Lüer, L.; Polli, D.; Cingolani, R.; Manna, L.; Lanzani, G. *Nano Lett.* **2008**, *8*, 4582−4587.
(32) Van Embden, J.; Jasieniak, J.; Mulvaney, P. *J. Am. Chem. Soc.* **2009**, *131*, 14299−14309.
(33) Ithurria, S.; Talapin, D. V. *J. Am. Chem. Soc.* **2012**, *134*, 18585−18590.
(34) Töben, L.; Gundlach, L.; Ernstorfer, R.; Eichberger, R.; Hannappel, T.; Willig, F.; Zeiser, A.; Förstner, J.; Knorr, A.; Hahn, P. H.; Schmidt, W. G. *Phys. Rev. Lett.* **2005**, *94*, 067601.
(35) Sasaki, F.; Mishina, T.; Masumoto, Y.; Fluegel, B.; Meissner, K.; Peyghambarian, N. *Semicond. Sci. Technol.* **1992**, *7*, B160.
(36) Hohenester, U.; Supancic, P.; Kocevar, P.; Zhou, X. Q.; Kütt, W.; Kurz, H. *Phys. Rev. B* **1993**, *47*, 13233.
(37) Rota, L.; Lugli, P.; Elsaesser, T.; Shah, J. *Phys. Rev. B* **1993**, *47*, 4226−4237.
(38) *II-VI and I-VII Compounds; Semimagnetic Compounds*; Madelung, O., Rössler, U., Schulz, M., Eds.; Landolt-Börnstein - Group III Condensed Matter; Springer-Verlag: Berlin/Heidelberg, 1999; Vol. *41B*.
(39) Ridley, B. K. *J. Phys. C Solid State Phys.* **1982**, *15*, 5899.
(40) Riddoch, F. A.; Ridley, B. K. *J. Phys. C Solid State Phys.* **1983**, *16*, 6971.
(41) Sippel, P.; Supplie, O.; May, M. M.; Eichberger, R.; Hannappel, T. *Phys. Rev. B* **2014**, *89*, 165312.
(42) Tessier, M. D.; Mahler, B.; Nadal, B.; Heuclin, H.; Pedetti, S.; Dubertret, B. *Nano Lett.* **2013**, *13*, 3321−3328.
(43) Algarte, A. C. S. *Phys. Rev. B* **1988**, *38*, 2162−2165.
(44) Wuister, S. F.; de Mello Donegá, C.; Meijerink, A. *J. Phys. Chem. B* **2004**, *108*, 17393−17397.
(45) Klimov, V. I.; McBranch, D. W.; Leatherdale, C. A.; Bawendi, M. G. *Phys. Rev. B* **1999**, *60*, 13740−13749.
(46) Klimov, V. I.; McBranch, D. W. *Phys. Rev. Lett.* **1998**, *80*, 4028−4031.
(47) Guyot-Sionnest, P.; Wehrenberg, B.; Yu, D. *J. Chem. Phys.* **2005**, *123*, 074709−074709−7.
(48) Nozik, A. J. *Annu. Rev. Phys. Chem.* **2001**, *52*, 193−231.
(49) Bockelmann, U.; Bastard, G. *Phys. Rev. B* **1990**, *42*, 8947−8951.
(50) Klimov, V. I.; Mikhailovsky, A. A.; McBranch, D. W.; Leatherdale, C. A.; Bawendi, M. G. *Phys. Rev. B* **2000**, *61*, R13349−R13352.

DOI: 10.1021/nl504706w
Nano Lett. 2015, 15, 2409−2416

(51) Grim, J. Q.; Christodoulou, S.; Di Stasio, F.; Krahne, R.; Cingolani, R.; Manna, L.; Moreels, I. *Nat. Nanotechnol.* **2014**, *9*, 891−895.

DOI: 10.1021/nl504706w
Nano Lett. 2015, 15, 2409−2416